

FLUID STRUCTURE INTERACTION PROBLEMS WITH CIRA STRUCTURED CFD SOLVER

DAVIDE CINQUEGRANA¹ AND PIER LUIGI VITAGLIANO²

¹ CFD Lab, Cira SCpA,
via Maiorise snc 80143 Capua (ITA)
d.cinquegrana@cira.it, www.cira.it

² CFD Lab, Head
via Maiorise snc 80143 Capua (ITA)
p.vitagliano@cira.it, www.cira.it

Key words: CFD, Multiphysics Problems, FSI, Computing Methods

Abstract. A multi-block structured flow solver[1] for unsteady RANS equations has been coupled with a structural solver within the software environment managed by the open source library preCICE[2], in order to perform fluid-structure interaction simulations.

Motivation of the work is the simulation of unsteady aerodynamic problems strongly dependent from structural behavior, like flexible aircraft, rotor-craft, counter-rotating rotors, etc.

Our CFD group has recently developed a system for flow simulation of unsteady compressible RANS equations based upon structured multi-block meshes, which allows the non-conformal block to block coupling (i.e. sliding mesh) and dynamic mesh on block base (i.e. some specific blocks in the flow field can be deformed and updated at each time step). Mesh is updated outside the flow solver, which makes possible to iterate with other systems to compute, in a segregated approach, structural deformation, body dynamics and possibly other physical phenomena.

This work shows the results of a verification test case and of the simulation of a panel flutter response at supersonic velocity, aiming to validate the whole process built up to face with fixed-point problem solution.

1 INTRODUCTION

A multi-block structured flow solver[3] for unsteady RANS equations has been coupled with a structural solver within the software environment managed by the open source library preCICE[2], in order to perform fluid-structure interaction simulations.

Motivation of the work is the simulation of unsteady aerodynamic problems strongly dependent from structural behavior, like flexible aircraft, rotor-craft, counter-rotating rotors, etc.

Our CFD group has recently developed a system for flow simulation of unsteady compressible RANS equations based upon structured multi-block meshes, which allows the

non-conformal block to block coupling (i.e. sliding mesh) and dynamic mesh on block base (i.e. some specific blocks in the flow field can be deformed and updated at each time step). Mesh is updated outside the flow solver, which makes possible to iterate with other systems to compute, in a segregated approach, structural deformation, body dynamics and possibly other physical phenomena.

Iterations can be performed in implicit mode, by repeating each time step with corrected meshes, in a loop controlled by convergence check outside the solver.

The flow simulation system communicates by delivering local forces on specific mesh surfaces, as specified in a set-up file, and it is capable to re-mesh the flow domain starting from a set of updated geometric entities like surfaces, curves and vertices, by following specific directives. Geometric entities can be specified or modified by control points.

Structural solver, already interfaced within the preCICE framework, is the open source FEM code Calculix[4]. As far as we know, this is the only CFD system based upon structured multi-block meshes fully integrated with a structural dynamic solver for unsteady simulations with dynamic meshes. The choice of the preCICE framework was driven by several reasons: the open source environment (no costs and limitations stemming from licences), easier implementation and shorter learning curve for using the structural solver, availability of both linear and non linear structural dynamic analysis, possibility of testing both explicit and implicit fluid-structure interaction, several interpolation and exchange methods for forces and deformations already available and implemented.

In the following sections the solvers are briefly described and the way they are interfaced in a segregated approach through preCICE dynamic library with some details on the CFD interface. Finally, results on two test cases are illustrated: one replicates test case available on the library documentation[5], while the other is a classical panel flutter investigation at supersonic speeds.

2 SEGREGATED APPROACH AND SOLVERS DESCRIPTION

The segregated approach to Fluid Structure Interaction problem can be a convenient strategy when well-validated solvers of the different involved physics models are already available, providing that those solvers communicate among them in an efficient way. In fact, there are relevant aspect that characterize the algorithms that manage the coupling among solvers. Those are specifically, the load and deformations transfer over the interfaces shared from the different computational domains, the time coupling of the different solutions to ensure convergence at each iteration and, finally, the way the solvers communicate information among them. Different approach adopted, characterize the several algorithms that are employed to face with a segregated approach. In this section the two solvers for fluid and structural domain are described: the former is ZEN, the CIRA finite volume structured multi-block solver. The latter, CalculiX, is an open source Finite Element Models field solver able to do linear and non-linear analysis of static and dynamic problems.

2.1 Aerodynamic Solver

ZEN is a multi-block structured flow solver for the U-RANS equations with classical ALE formulation. It is based upon second-order finite volumes central schemes, cell-centered spatial discretization, and second order backward implicit time discretization. Convergence in each time step is achieved with dual time stepping through explicit Runge-Kutta multi-stages, and acceleration techniques like local time stepping, residual averaging and multi-grid. Non conformal conservative internal boundary conditions for moving surfaces can be applied for rigid mesh movement (sliding mesh). Dynamic meshes are implemented by following the 3 step backward implicit time scheme in such a way to satisfy the discrete geometrical conservation law (DGCL[6]). The updated mesh is reloaded at each time step, which allows to post-process surface deformations due to structural dynamics or to body dynamics outside the flow solver. The current time step can be repeated (and the updated mesh reloaded), when required, under control of external routines that check for suitable convergence criteria, as it is necessary in case of implicit fluid-structure interaction. It is possible to apply dynamic mesh modifications only in some blocks, to save computational time. The flow solver communicates at every time step with other systems by producing a table of global loads on selected surfaces (the so-called faces) and a set of files containing selected surfaces with local force distributions at each mesh point, sum of pressure and friction contributions.

2.2 Structural Solver

CalculiX is the open source solver employed to carry out non-linear analysis of dynamic problems as already interfaced to the preCICE library. In detail, to calculate the non-linear response of a structure subject to dynamic loading an implicit integration procedure of the equations of motion is employed. The implicit solver uses Incomplete Cholesky pre-conditioning and the iterative solver by Rank and Ruecker [7], which is based on the algorithms by Schwarz [7]. This solver is well suited for shell elements as indicated by the author.

The equation of motion is integrated in time using the α -method developed by Hilber, Hughes and Taylor[7]. The α parameter lies in the interval $[-1/3,0]$ and controls the high frequency dissipation: $\alpha=0$ corresponds to the classical Newmark method inducing no dissipation at all, while $\alpha=-1/3$ corresponds to maximum dissipation[7].

3 FLUID STRUCTURE COUPLING

This section describes the way CFD and FEM solvers are coupled in a segregated approach. From the structural side, the architecture illustrated from Rush[2] is adopted, i.e. the Calculix solver has its adapter that exchanges data with CFD solver through preCICE library. From the CFD solver side, we developed a black-box adapter coupled with a bash script that is able to manage the timing processes and the ZEN-interface with preCICE.

The coupling between the two solvers is managed by the open-source preCICE library. The library is able to treat the numerical methods for equation's coupling, methods to

interpolate data in the frame of load transfer and methods to communicate among the different solvers involved in the multi-physics simulations. Hence, we have to configure the library to deal with the proposed test case, according also to the way we have developed the interface of the aerodynamic solver. The configuration is executed at runtime via an xml file where the solvers, the fluid and solid interfaces that are exchanging data, the kind of data (i.e. scalars, vectors) are tagged. Here are set also the mapping of loads according to the direction the data are going to: i.e. from the fluid solver to the structure one and vice-versa. Into the configuration file are defined the interpolator (RBF, Nearest-Neighbor, Nearest-Projection) and the constraint type employed in the load transfer that ensure for conservativeness if data go from CFD to FEM, and consistency if they go from FEM to CFD.

Since the library interface we developed is a black-box with respect to the CFD solver, the communication in the FEM - library direction is only managed by the library: this is configured with a point-to-point based on TCP/IP socket. The communications in CFD to preCICE direction, as illustrated in next section, is based on file-transfer.

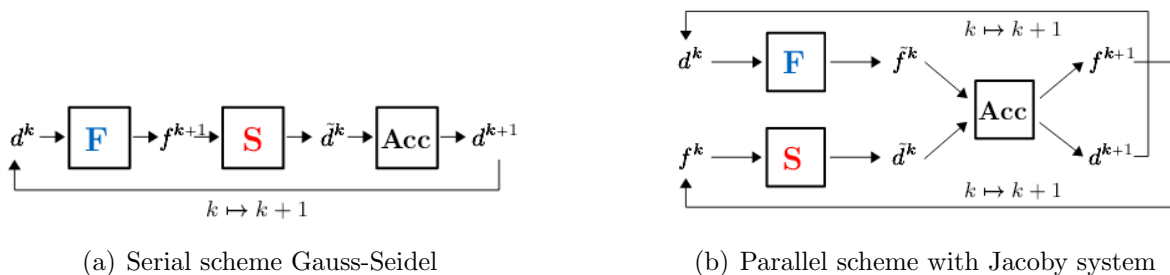


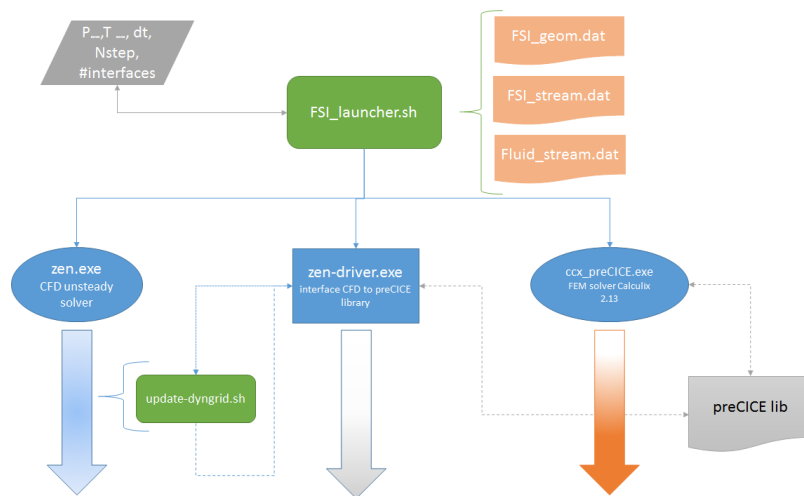
Figure 1: Flow Chart of coupling scheme for fixed point problem solution[5]

Finally the coupling scheme among the participants has to be set. In the preCICE library both explicit schemes, that compute a single solver computation in one time-step, and implicit schemes, that sub-iterate until convergence, shown in Figure 1 are available. For the latter approach, preCICE offers acceleration schemes, such as a simply (dynamic) under-relaxation (or Aitken), but also sophisticated quasi-Newton schemes as the IQN-ILS scheme (also known as Anderson acceleration) and the IQN-MVJ scheme (also known as generalized Broyden).

3.1 CFD ZEN INTERFACE

The structured ZEN code is coupled with the FEM solver Calculix through the preCICE library. From the FEM side, CalculiX exchanges data with preCICE through a devoted interface[2, 5, 8]. In this section the way the CFD ZEN solver exchanges data with preCICE is described.

Figure 2 illustrates conceptually how the FSI analysis starts and how data are exchanged during the calculation between the ZEN CFD solver and the ZEN interface: the latter sends data to preCICE.


Figure 2: Global chart

The ZEN-driver interface is coded in cpp language. It is aimed to share the CFD variables (i.e. the non-dimensional loads), available after a CFD time step, with the preCICE library, that in turn, communicates with the FEM solver adapter. When launched, the ZEN-driver employs the information about free-stream values, calculating the dimensional loads.

The simulation starts by launching a shell script that manages the initialization step. At the beginning the script reads the input of the two solvers, in order to compute the data required to match the right dimensions.

As the CFD code ZEN solves non-dimensional equations, reference dimensions are required in order transform local and global forces, i.e. static pressure and static temperature, time step and scale length. Moreover, the interface reads information about the face numbering for the exchange of local loads, those have to match the structural mesh.

At every time step ZEN computes local loads on each face to be exchanged with preCICE, then it issues a message and waits for updated surfaces. When preCICE has produced the surfaces updated with the new structural deformations, it sends ZEN a signal to inform whether the time step has reached the convergence or it should be repeated with the new surfaces. In both cases the flow solver system generates a new mesh and then the computation proceeds following the directive.

In Figure 3 are illustrated the stream of data during the communication from the CFD solver and the ZEN interface, through the script named update-dyngrid.sh. This 'black box' approach can be efficient and fast, but it presents some drawbacks (i.e. it does not share data with mpi or socket communication, but only with files).

ZEN CFD solver and the ZEN-driver interface are running at same time: when a CFD time step is completed, the solver calls the script update-dyngrid.sh. Within this script, loads data available over the interface are sent to the FEM solver through the dynamic library preCICE. At this point the script waits until the displacements data are sent back: once those are ready, a new grid is computed and a new time step calculation

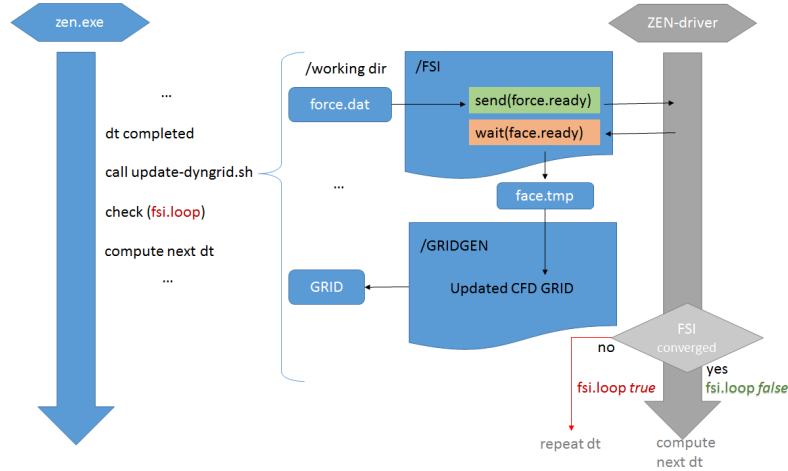


Figure 3: Detailed update-dyngrid.sh procedure chart

starts. The procedure is different when the algorithm foresees sub-iterations, i.e. when a strong coupling approach is chosen. In this case, until the sub-iteration convergence is not reached, the ZEN-interface informs the flow solver to repeat the same time step through the `fsi.loop` flag.

4 RESULTS

4.1 Verifying Test Case

This section describes a test case set up to verify that the whole process works properly, by simulating a deformable flap and comparing the results with those obtained using SU2 as CFD code, already coupled with Calculix, through the preCICE library[2]. The simulation aims to verify qualitatively the correct work-flow of the data process, so we do not analyze in detail the numerical results, as no experimental data are available for comparison.

The CFD domain is shown in Figure 4 (a), the channel height is 2 m, while the flap is characterized by height, $h_f = 1.6$ and width, $w_f = 0.2$. The domain extend 10 m before and after the flap, and it is discretized with 3 blocks and 9224 cells.

The material and physical parameters of the simulation are different from those shown in the thesis of Rusch[8]: the free-stream Mach and Reynolds number are respectively 0.1 and 10.0^6 , while pressure and temperature are $p_\infty = 144900[Pa]$, $T_\infty = 288.4[K]$. The structural parameter values are the density $\rho = 10^5 Kg/m^3$, Poisson ratio $\nu = 0.33$ and Young modulus $E = 10^9 N/m^2$. Regarding the simulations settings, time-step length is $10^{-4}(s)$. The mapping method consists of RBF-volume-splines, with a serial-implicit coupling using Aitken relaxation. Maximum number of sub-iterations allowed in one single time step is 10.

In Figure 4 (b) are shown streamlines and stream-wise velocity component surrounding moving flap during in the FSI simulation.

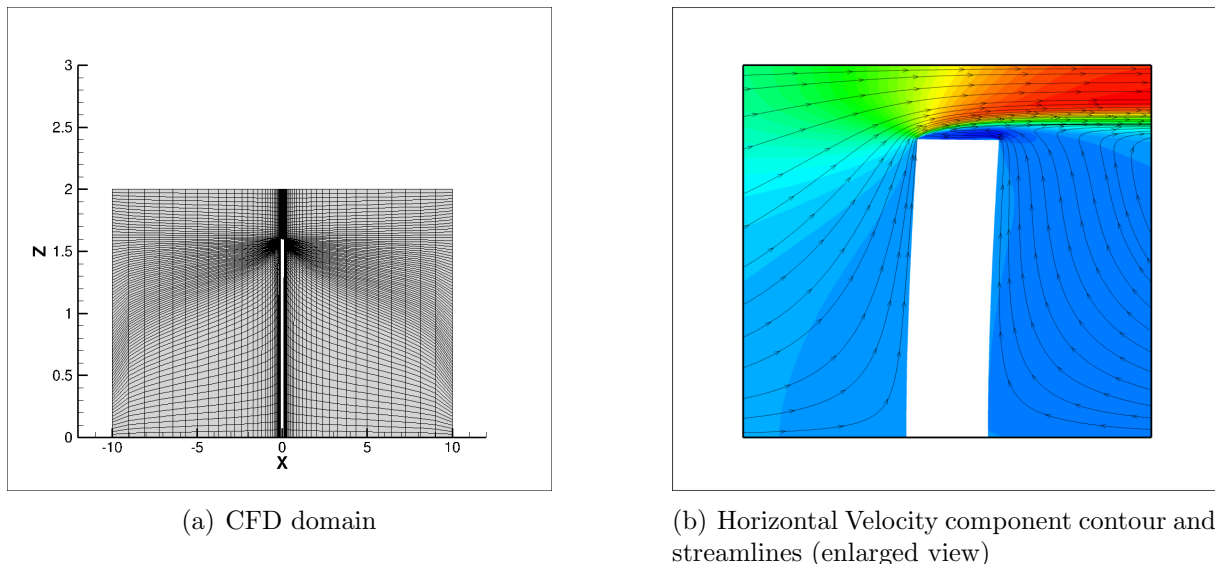


Figure 4: Oscillating Flap

4.2 Validation Test Case: Supersonic Panel Flutter

To evaluate the performance of such a coupled algorithm, we consider a two-dimensional simulation of a transient non-linear aero-elastic response of a flat panel in a supersonic stream. In details, the panel is fixed at both ends, and the free stream Mach number is set to $M_\infty = 2.3$, the panel length is $a = 0.5$ (m) with uniform thickness $h = 1.35 \times 10^{-3}$ m. The structural parameter values are density $\rho_m = 2710 \text{ Kg/m}^3$, Poisson ratio $\nu = 0.33$ and Young modulus $E = 77.281 \times 10^9 \text{ N/m}^2$. This condition is expected to be quite near to flutter [9, 10, 11].

The problem of instability of plates in gas flow has been widely investigated. In supersonic flow, the instability has the oscillatory nature known as flutter, that can be distinguished in coupled or single-mode flutter [12]. Several time-domain simulations of non-linear panel flutter were performed from transonic to supersonic flows by several authors [9, 13, 12, 14]. From their results at high Mach number flows we should expect high frequency Limit Cycle Oscillations (LCO) and non periodic oscillations.

Here we investigate how the amplitude and the frequency of the LCO changes, according to the critical dynamic pressure, λ , defined as $\lambda^* = \frac{\rho_\infty u_\infty^2 a^3}{D}$, where D is the plate stiffness, $\frac{Eh^3}{12(1-\nu^2)}$. Hence, by changing the Young modulus of the plate, we have obtained a set of λ^* values at which the analysis are carried out. The mass ratio, μ , calculated as $\mu = \frac{\rho_\infty a}{\rho_m h}$, is kept constant during the simulations and equal to 0.055. The plate, is modeled with quadratic shell elements with 8 nodes, 34 elements stream-wise and just 2 elements span-wise. The edges are fully constrained, while in the plane of symmetry the in-plane displacements and rotations are allowed.

In order to compare the results with other authors without the uncertainties stemming from boundary layer (BL) thickness and turbulence model effects, the flow is solved with Euler equations. The CFD grid, shown in Figure 5, is made of one block with 112×80

cells, and has 35 nodes on the interface. As the two meshes are quite comparable on the interface, we do not expect large differences in the results due to the load transfer process, as we can see in the next sections.

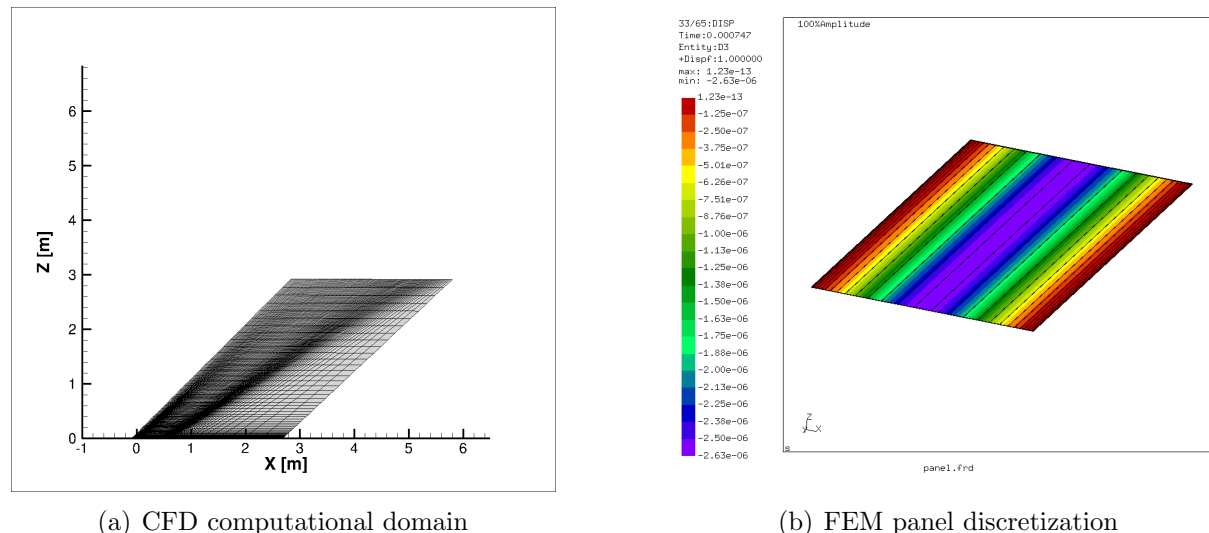


Figure 5: CFD grid

The two solvers starts together the integration from free-stream values, and an initial vertical velocity is assigned to the flat panel, equal to $\delta w = w_0 \sin^2\left(\frac{\pi x}{L}\right)$ where w_0 , is a constant suitable to produce an initial perturbation.

4.2.1 preCICE interface library settings

In this run, we have compared the results of two interpolation type: Radial Basis function with Thin Plate Splines and Nearest-Neighbor.

The nature of the problem under investigation requires a strongly coupled approach, hence we chose an implicit scheme, the classical fixed-point system based on a Gauss-Seidel execution of both solvers (or serial coupling). As acceleration technique a dynamic Aitken under-relaxation is adopted. The initial relaxation value is 0.01 and an extrapolation of order 2 is used as initial guess in every iteration. In future works, those results will be compared with the parallel coupling scheme (a Jacoby vectorial scheme) with more complex quasi-Newton schemes as post-processing or accelerator (already available within the preCICE library).

The relative convergence threshold values for displacements and forces are different, and chosen in a trial and error approach: they are, for displacement 10^{-2} , and for forces 10^{-3} .

Even if the preCICE library is able to manage non-matching discretization in time relative to the different solvers, in our simulations the "first participant" approach is adopted, hence the time-step is imposed by the CFD solver, and the FEM solver takes the same value.

An investigation was conducted, and shown in next subsection, to set the correct time step length in a time convergence analysis, where this is varied until to reach a stable solutions.

4.2.2 Time solution dependency

This analysis shows that, even if the simulations are carried out with a fully-implicit approach (i.e. with sub-iterations), the time-step plays a key role in capturing the higher frequency eigen-modes at which the panel oscillates.

In Figure 6 the time histories of vertical displacement at a fixed panel point are shown, for different time steps, at different dynamical pressure, λ^* . It can be seen that, whatever the λ^* is, by diminishing the time step, the total time of simulation up to the divergence increases, and the behavior of the oscillations is changing, capturing well the switch to another limit cycle.

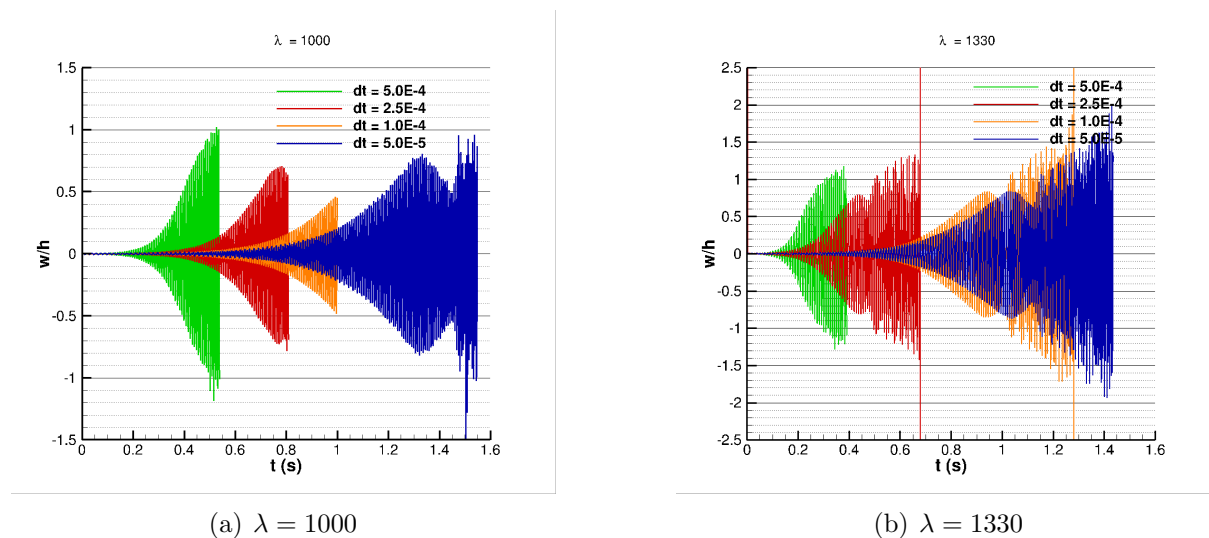


Figure 6: Time history of vertical displacement, (w/h) at $x/a=0.75$ for different time steps length.

Figure 7 shows that, with a smaller dt , some instabilities on the maximum and minimum point positions are better captured.

In the next subsection, where the LCO behavior is analyzed by varying the dynamic pressure λ^* , the smallest time-step is chosen.

4.2.3 Limit Cycle Oscillations

The instability of plates has been investigated in numerous studies in the context of panel flutter: in the case of supersonic flow, the nature of instability can be either coupled or single mode flutter[12]. In this work we have found the switching to different limit cycles during the simulations. Since the attention is restricted to the development and validation of the coupling system for the analysis of FSI problems, the stability boundaries are not

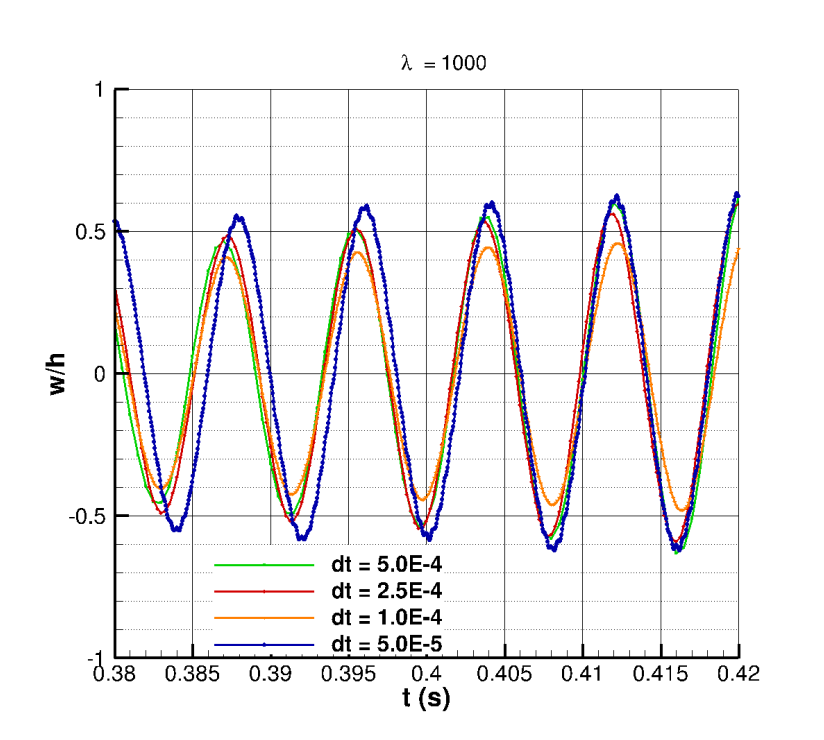


Figure 7: Zoom on time history of vertical displacement, (w/h) at $x/a=0.75$ for different time steps length, $\lambda = 1000$

investigated in detail, but a few points with different free-stream dynamic pressure λ^* and relative LCO are reported.

At the Mach number considered in these calculations, it is noted that, to establish an asymptotic limit-cycle response, longer time would be required: as it was explained also in the work of Gordnier et al.[13], the reason is that the final flutter response involves higher panel modes (see Figure 8). In our test cases, all carried out with the time-step of 1.0×10^{-5} s, the simulations start with an initial perturbation velocity on the FEM nodes and free-stream flow velocities on undeformed panel.

The initial velocity law imposed to the FEM nodes is related to the first proper mode of deformation for this kind of panel configuration and boundary conditions (clamped, 2D). Hence, the panel starts to oscillate in the way of the first mode, and under the effects of aerodynamic loads the higher modes are excited, becoming predominant to the lowest ones: this takes a long simulation time. Figure 8 reports on the left the time history of vertical displacement of a point located at $x/a=0.75$, and on the right the relative oscillation frequency, normalized with the fundamental linear frequency of the plate, $\omega_0 = \pi^2 \sqrt{\frac{D}{\rho_m h a^4}}$.

From the displacement plots, it can be seen that the flutter does not start immediately, and that the simulations interrupt just before the oscillations become periodic, due to divergence, considering that the maximum number of sub-iterations of the implicit coupling (set at 30), is reached more or less at the same physical time, whatever the critical

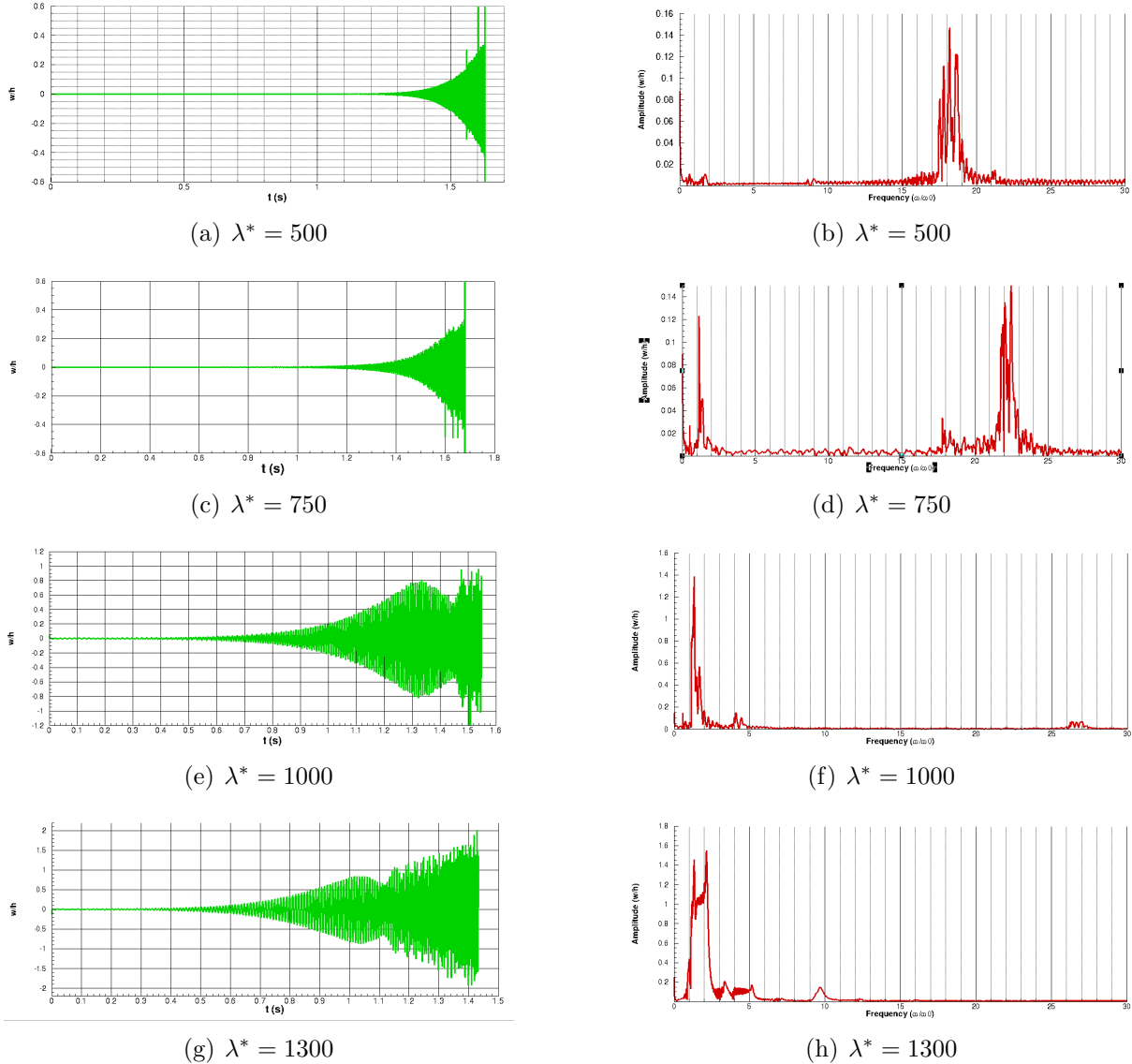


Figure 8: Flutter response at $x/a=0.75$ for $M_\infty=2.3$, $dt=1.0 \times 10^{-5}$ (s)

freestream pressure value. Furthermore, in the cases of $\lambda^* = 1000, 1330$, the switching from one mode to another during the oscillations can be clearly seen: such phenomena highlighted also from Shishaeva [12]. The frequency spectra reveal that higher modes are concurring in the way the panel deforms and oscillates. Those spectra changed during the simulations, since at the beginning, the most important frequency are the lower ones, while the higher ones are not detected.

Figure 9 shows flow solutions at two different times: in the first one a strong incident shock wave in the middle of panel, while the other shows an expansion at the same location.

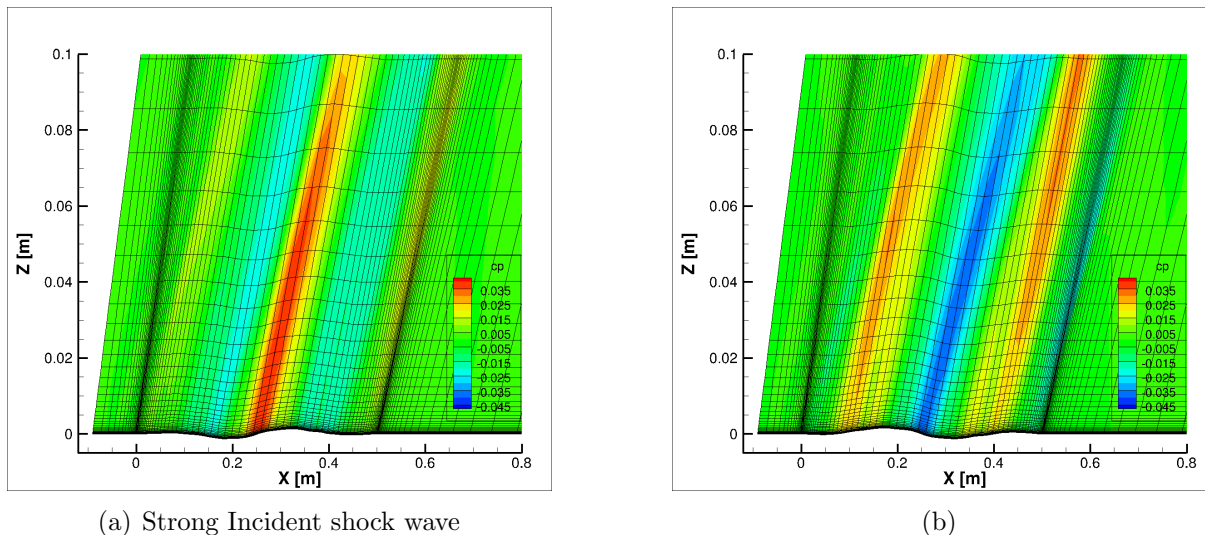


Figure 9: Euler flow field solutions for $\lambda = 1330$, $dt = 1.0e^{-4}$

4.2.4 Impact of Turbulent Boundary Layer

In literature few simulations are available on the influence of turbulent BL on the aero-elastic behavior of a panel. It is known that laminar BL induces significant damping effects at low supersonic Mach number[13]. In the work of Alder[15], also the effects of 2D and 3D simulations are investigated, with $k - \omega$ SST models for turbulent BL. He finds that exceeding Mach 1.6 the impact becomes less significant, and the dependence of λ^* for flutter onset shows a linear behavior with respect to the BL thickness[15].

A Navier-Stokes solutions was obtained for Reynolds number of $Re = 18.10^6$, with the two equation Menter $k - \omega$ SST model, available in the CIRA ZEN code [16]. At the beginning of FSI simulation with flow developed on the undeformed panel configuration, the BL thickness is with $\frac{\delta_{99}}{a} = 0.36$ at mid panel.

The FEM models is the same adopted in the other numerical tests. A difference can be found in the way the FSI analysis starts: at the beginning the plate is kept fixed while the flows develops. Then, after some time steps integrated by CFD, the FEM starts its calculations, taking the loads coming from CFD.

Figure 10 shows damping effects of boundary layer obtained by the NS simulations with SST turbulence model. Those results are relative to a time-step of $5.0 \times 10^{-4}(s)$.

4.3 Effects of spatial load transfer methods

One critical aspect of an FSI problem, is the ability of the two subsystems of exchanging energy without loss (or production): the loads computed and transfered through the interfaces should verify this conservative property. Then, a conservative interpolation algorithm for load transfer between the interfaces is mandatory. In several works is remarked that the consistency property in translating the displacements from FEM to CFD has also a key role[17, 18, 19, 20]. Here, two different interpolation algorithms are compared: the Nearest-Neighbor and the Radial Basis Function-TPS, both in the

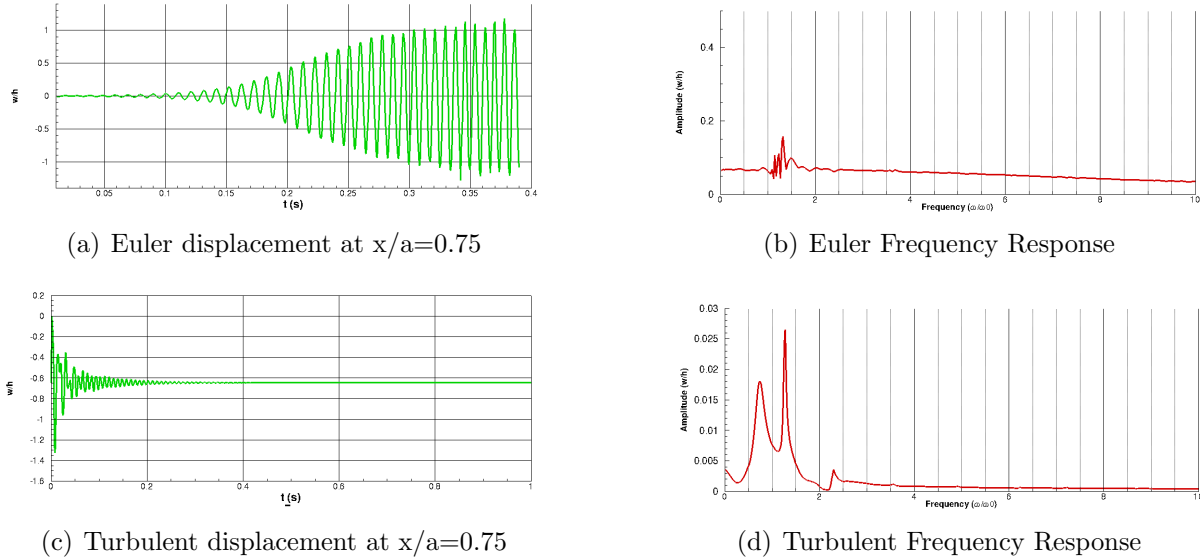


Figure 10: Turbulent Boundary Layer effects on panel flutter LCO, $\lambda^* = 1300$

conservative formulation when forces are transferred from CFD to FEM, and in consistent formulation, when displacement are mapped from FEM to CFD.

As seen in previous section, with turbulent BL at $\lambda = 1330$, the plate reaches an equilibrium position in a deformed shape. Figure 11 shows in a time-window how the time history of the diverged panel is changing, if the load transfer is executed with NN or RBF-TPS: the panel is oscillating at same frequency but the equilibrium position reached by RBF is slightly lower with respect to NN load interpolation.

Figure 12 shows panel shapes at different point of time-history with a circular symbols located at the reference point for used in the LCO analysis: Figure 12 (a) is relative to NN interpolation, while Figure 12 (b) is relative to the RBF-TPS.

Aknowledgement

The authors wish to thank Dr Uekermann and the whole preCICE staff for their support and advices.

5 CONCLUSIONS

This paper has described the development of an interface that glues the CIRA ZEN CFD code with an open source FEM code by means of the preCICE library. After verified that the developed coupling process works with a first test case, the classical FSI problem of a panel flutter at supersonic speed has been simulated with a strongly-coupled partitioned approach. The results are encouraging, even if they only be considered as preliminary, demonstrating that the partitioned approach between the structured CFD solver and FEM is possible through preCICE library. In order to optimize the efficiency of the process, future works will consider the implementation of mpi or TCP/IP communications, and testing different coupling schemes for the fixed point problem solution.

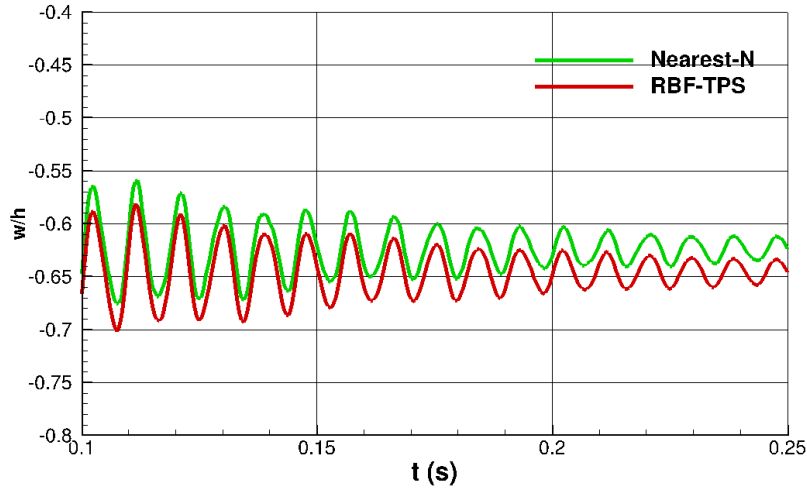


Figure 11: Displacement at 0.75 of panel length - NN vs RBF

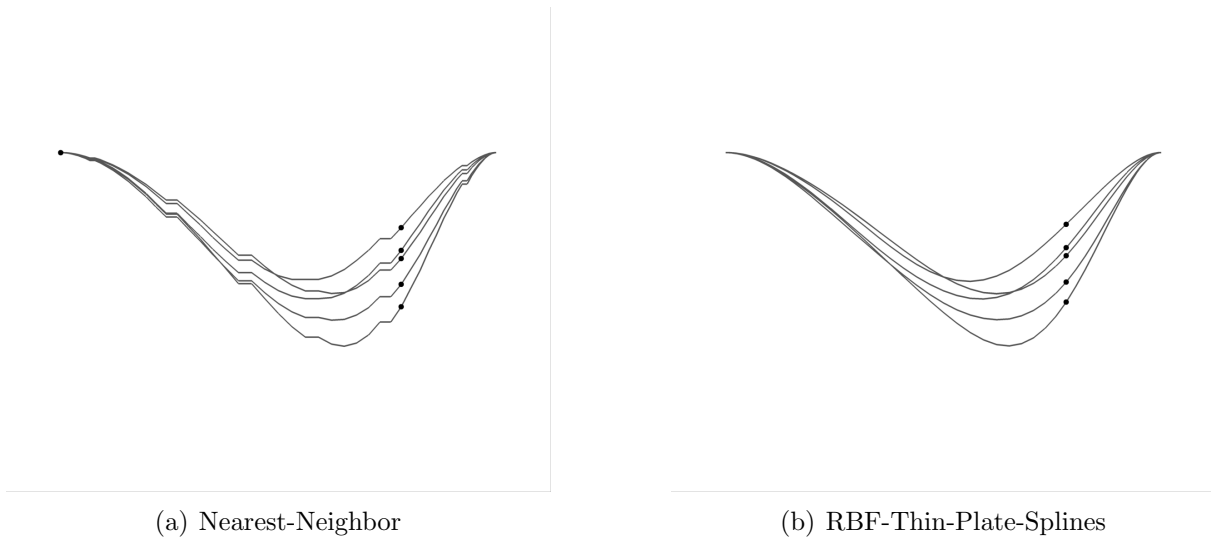


Figure 12: Deformed panel shapes at different time-step: results of different load transfer interpolation coupling

REFERENCES

- [1] Marongiu C, Catalano P, A. M. e. a., “U-ZEN: a computational tool solving U-RANS equations for industrial unsteady applications,” *34th AIAA fluid dynamics conference, Portland OR*, No. AIAA Paper 2004-2345, 2004.
- [2] Bungartz, H.-J., Lindner, F., Gatzhammer, B., Mehl, M., Scheufele, K., Shukaev, A., and Uekermann, B., “preCICE – A Fully Parallel Library for Multi-Physics Surface Coupling,” *Computers and Fluids*, Vol. 141, 2016, pp. 250—258.
- [3] Vitagliano, P. L., Minervino, M., Quagliarella, D., and Catalano, P., “A conservative

- sliding mesh coupling procedure for U-RANS flow simulations,” *Aircraft Engineering and Aerospace Technology*, Vol. 88, No. 1, 2016, pp. 151–158.
- [4] Dhondt, G., *The Finite Element Method for Three-Dimensional Thermomechanical Applications*, Wiley, 2004.
- [5] Uekermann, B., *Partitioned Fluid-Structure Interaction on Massively Parallel Systems*, Dissertation, Institut für Informatik, Technische Universität München, Oct. 2016.
- [6] Farhat, C., Lesoinne, M., and LeTallec, P., “A conservative algorithm for exchanging aerodynamic and elastodynamic data in aeroelastic systems,” *Aerospace Sciences Meetings*, American Institute of Aeronautics and Astronautics, Jan. 1998, pp. –.
- [7] Dhondt, G., *CalculiX CrunchiX USER’S MANUAL version 2.13*, 08 2017.
- [8] Rusch, A., *Extending SU2 to fluid-structure interaction via preCICE.*, Master’s thesis, Munich School of Engineering, Technical University of Munich, 2016.
- [9] DAVIS, G. and BENDIKSEN, O., “Transonic panel flutter,” *Structures, Structural Dynamics, and Materials and Co-located Conferences*, American Institute of Aeronautics and Astronautics, April 1993, pp. –.
- [10] Farhat, C., “Load and motion transfer algorithms for fluid/structure interaction problems with non-matching discrete interfaces: Momentum and energy conservation, optimal discretization and application to aeroelasticity,” *Computer Methods in Applied Mechanics and Engineering*, Vol. 157, 1998, pp. 95–114.
- [11] Farhat, C. and Geuzaine, P., “Design and analysis of robust ALE time-integrators for the solution of unsteady flow problems on moving grids,” *Computer Methods in Applied Mechanics and Engineering*, Vol. 193, No. 39, 2004, pp. 4073 – 4095, The Arbitrary Lagrangian-Eulerian Formulation.
- [12] Shishaeva, A., Vedeneev, V., and Aksenov, A., “Nonlinear single-mode and multi-mode panel flutter oscillations at low supersonic speeds,” *Journal of Fluids and Structures*, Vol. 56, 2015, pp. 205 – 223.
- [13] GORDNIER, R. and VISBAL, M., “DEVELOPMENT OF A THREE-DIMENSIONAL VISCOUS AEROELASTIC SOLVER FOR NONLINEAR PANEL FLUTTER,” *Journal of Fluids and Structures*, Vol. 16, No. 4, 2002, pp. 497 – 527.
- [14] Hashimoto, A., Aoyama, T., and Nakamura, Y., “Effects of Turbulent Boundary Layer on Panel Flutter,” *AIAA Journal*, Vol. 47, No. 12, Dec. 2009, pp. 2785–2791.
- [15] Alder, M., “Development and Validation of a Partitioned Fluid-Structure Solver for Transonic Panel Flutter with Focus on Boundary Layer Effects,” *AIAA AVIATION Forum*, American Institute of Aeronautics and Astronautics, June 2014, pp. –.

- [16] Catalano, P. and Amato, M., “An Evaluation of RANS Turbulence Modeling for Aerodynamic Applications,” *Aerospace Science and Technology*, Vol. 7, No. 7, 2003, pp. 493–590.
- [17] Cebal, J. R. and Lohner, R., “Conservative Load Projection and Tracking for Fluid-Structure Problems,” *AIAA Journal*, Vol. 35, No. 4, April 1997, pp. 687–692.
- [18] Farhat, C., Lesoinne, M., and Tallec, P. L., “Load and motion transfer algorithms for fluid/structure interaction problems with non-matching discrete interfaces: Momentum and energy conservation, optimal discretization and application to aeroelasticity,” *Computer Methods in Applied Mechanics and Engineering*, Vol. 157, No. 1, 1998, pp. 95 – 114.
- [19] Jaiman, R., Geubelle, P., Loth, E., and Jiao, X., “Transient fluid-structure interaction with non-matching spatial and temporal discretizations,” *Computers and Fluids*, Vol. 50, No. 1, 11 2011, pp. 120–135.
- [20] de Boer, A., van Zuijlen, A., and Bijl, H., “Comparison of conservative and consistent approaches for the coupling of non-matching meshes,” *Computer Methods in Applied Mechanics and Engineering*, Vol. 197, No. 49, 2008, pp. 4284 – 4297.